Global dynamics for a non-smooth Filippov system with the threshold strategy

Yuxun Zhu
Jiangsu University
Lu Liu
Jiangsu University
Zhengdi Zhang (dyzhang@ujs.edu.cn)
Jiangsu University

Research Article

Keywords: IPM, Filippov systems, Economic threshold, Sliding mode, Global stability

Posted Date: May 7th, 2021

DOI: https://doi.org/10.21203/rs.3.rs-455999/v1

Nonlinear Dynamics manuscript No.
(will be inserted by the editor)

Global dynamics for a non-smooth Filippov system with the threshold strategy

Yuxun Zhu · Lu Liu · Zhengdi Zhang

Received: date / Accepted: date

Abstract In this study, the Leslie-Gower model with functional response is extended into a non-smooth Filippov system by applying IPM strategies. Once the number of pests reaches or surpasses the given economic threshold(ET), spraying pesticides and releasing the natural enemy are implemented simultaneously. In order to maintain the pest population at or below ET, global dynamics of the proposed model are investigated completely, including the existence of sliding mode and various equilibria, sliding dynamics and global stability of equilibria. The result shows that real equilibrium cannot coexist with the unique pseudo-equilibrium. In particular, after excluding the existence of any possible limit cycle, the global stability of equilibria is obtained by employing qualitative and numerical techniques. In the end, the effect of our work on pest control are discussed.

Keywords IPM · Filippov systems · Economic threshold · Sliding mode · Global stability

1 Introduction

It is well-known that insects play an important role in ecological balance, but some of them collectively referred to as pests would have a substantial adverse impact on human life[1–3]. This is especially conspicuous in agriculture. Once the number of pests exceeds a certain value, causing infestation, it is bound to bring about an immeasurable loss to crop yield, crop quality, together with social economy. Therefore, pest management has been always a hot spot for many scholars[4–6]. During the World War II, some organochlorine insecticides, such as DDT, were found to be effective in controlling pests, but the long-term abuse of these chemical pesticides can lead to insect resistance, environmental pollution and even the resurgence of secondary pests due to the damage of pesticides to natural enemies[7–9]. According to the survey report from U.S. department of agriculture[10], although the dosage and concentration of pesticides used in agriculture in the United States increased tenfold respectively between 1940 and 1978, the loss of crop yield went up from 7% to 17% and the quantity of pests rose as well. So it was gradually realized that using chemical methods alone was not feasible, and the concept of IPM(Integrated Pest Management) came up in the meantime. IPM is aimed at integrate suitable measures, such as chemical and biological methods, to manage the number of pests below EIL(Economic Injury Level) instead of killing off them, thereby not only avoiding economic losses but also contributing to the sustainable development of agroecosystem[11–13]. Actually, taking measures when the number of pests approaches to EIL cannot prevent the economic toll timely, so the Economic Threshold(ET<EIL) is set as a critical value, that is, once the pest population reaches or exceeds ET, appropriate measures should be applied to reduce the quantity below ET, which can ensure that EIL is never possible for the pest population to reach.

There have been many mathematical models established to investigate the efficiency of IPM strategies, including fixed moment and state-dependent impulsive differential equations[14–16]. However, some weaknesses of this class of models can be noticed. For the former, control strategies are implemented at the fixed moment regardless of whether the pest population reaches ET,

Yuxun Zhu · Lu Liu · Zhengdi Zhang
Department of Mathematics, Jiangsu University, Zhenjiang 212013, China
Corresponding author: Zhengdi Zhang
E-mail: dyzhang@ujs.edu.cn

which can enhance the cost and cause a waste of resources. And for the latter, they assume that the death of pests is an instantaneous process, whereas this process is continuous in reality[17]. Hence, compared with above models, the non-smooth Filippov system is more realistic as it means that once the quantity of pests surpasses ET, continuous control measures will be taken until it falls below ET again. Recently, Filippov systems with the threshold policy have been extensively investigated[18–23]. But referring to Filippov predator-prey ecosystems therein, it is interesting to note that very few previous studies have considered carrying capacity of the predator. So in this paper, we will use the Leslie-Gower(LG) model with Holling type I functional response to describe the interaction between pests and natural enemies[24]:

$$\begin{cases} \dfrac{dx}{dt} = rx\left(1-\dfrac{x}{K}\right) - mxy, \\ \dfrac{dy}{dt} = y\left[s\left(1-\dfrac{hy}{x}\right)\right], \\ x(0)>0,\ y(0)>0,\ r,s,h,K>0, \end{cases} \tag{1}$$

where x and y represent the population of pests and natural enemies, r and s are the intrinsic growth rates of the pest and the natural enemy respectively, the functional response mx indicates the consumption of the natural enemy to the pest; although pests and natural enemies both grow logistically, carrying capacity of the pest is a constant K while that of the natural enemy is proportional to the pest population.

When the number of pests is less than ET, no control measure is carried out and the model(1.1) holds true. But as long as the pest population reaches or surpasses ET, we will apply IPM strategies to spray insecticide and release natural enemy simultaneously, and then the following extended LG model with IPM strategies is set up:

$$\begin{cases} \dfrac{dx}{dt} = rx\left(1-\dfrac{x}{K}\right) - mxy - p_1x, \\ \dfrac{dy}{dt} = y\left[s\left(1-\dfrac{hy}{x}\right)\right] + p_2y, \end{cases} \tag{2}$$

where the killing rate of pests and the release rate of natural enemies are expressed by p_1 and p_2 separately. Consequently, the combination of models (1.1) and (1.2) is the Filippov system which we will investigate in the rest of this paper.

Throughout this paper, in order to guarantee the existence of internal equilibria and sliding mode, we assume $r > p_1$, which means that the killing rate caused by spraying pesticide is less than the intrinsic growth rate of pests; moreover, $K > \frac{rET}{r-p_1}$ is assumed, which also ensures the normal survival of the pest population in the ecosystem and makes the implementation of our control strategies needed and meaningful.

Our main purpose of this study is to probe into the global dynamics of model (1.1) with (1.2). Hence in section 2, we first give a detailed explanation of our Filippov system and present some useful preliminaries. Afterwards, dynamical behaviors of models (1.1) and (1.2) are investigated separately. In section 3, we exhibit sliding mode dynamics and the existence of five types of equilibria. Furthermore, local stability of pseudo-equilibrium is analyzed. In section 4, the global dynamics are obtained based on the previous discussion, and the results of numerical simulation are shown to verify theoretical analysis. At last, biological implications are provided in section 5.

2 Preliminary results

We apply the threshold policy into LG model in order to manage the pest population more appropriately, and then the combination of models (1.1) and (1.2), namely the Filippov system, is acquired as follows:

$$\begin{cases} \dfrac{dx}{dt} = rx\left(1-\dfrac{x}{K}\right) - mxy - \gamma p_1 x \doteq f_1, \\ \dfrac{dy}{dt} = y\left[s\left(1-\dfrac{h}{x}y\right)\right] + \gamma p_2 y \doteq f_2, \end{cases} \tag{3}$$

with

$$\gamma = \begin{cases} 0, & x - ET < 0, \\ 1, & x - ET > 0, \end{cases} \tag{4}$$

where p_1x represents the impact on pest population caused by chemical method, spraying insecticides, and p_2y is the number of releasing natural enemies.

Due to the property of this model, let $D = \{(x,y) \in R | x > 0, y \geq 0\}$ be the field of definition of system(2.1) with (2.2). Then denote Z=(x,y), a smooth scale function H(Z)=x-ET and

$$F_1(Z) = (f_{11}(Z)\ ,\ f_{12}(Z))^T\ ,\ F_2(Z) = (f_{21}(Z)\ ,\ f_{22}(Z))^T\ ,$$

where

$$\begin{aligned} f_{11}(Z) &= rx\left(1-\frac{x}{K}\right) - mxy, \\ f_{12}(Z) &= y\left[s\left(1-\frac{h}{x}y\right)\right], \\ f_{21}(Z) &= rx\left(1-\frac{x}{K}\right) - mxy - p_1x, \\ f_{22}(Z) &= y\left[s\left(1-\frac{h}{x}y\right)\right] + p_2y. \end{aligned}$$

Hence, the system(2.1) and (2.2) can be rewritten as a generalized Filippov system shown below:

$$\dot{Z} = \begin{cases} F_1(Z) & Z \in S_1, \\ F_2(Z) & Z \in S_2, \end{cases} \tag{5}$$

where $S_1 = \{Z \in D \mid H(Z) < 0\}$ and $S_2 = \{Z \in D \mid H(Z) > 0\}$. In particular, the discontinuous boundary between the region S_1 and S_2 is defined as $\Sigma = \{Z \in D | H(Z) = 0\}$, so we have $D = S_1 \cup \Sigma \cup S_2$. In the following, we call the system(2.3) defined in the region S_1 or S_2 as subsystem F_1 or subsystem F_2 respectively.

For the discontinuous boundary Σ, it can be segmented into the following regions:

(i) Sliding region Σ_S: $\langle F_1(Z), H_Z(Z)\rangle > 0$ and $\langle F_2(Z), H_Z(Z)\rangle < 0$ hold true, which means that trajectories that once touch Σ_S will stay on it,

(ii) Crossing region Σ_C: $\langle F_1(Z), H_Z(Z)\rangle \langle F_2(Z), H_Z(Z)\rangle > 0$ holds true, which implies that trajectories can pass through Σ_C to another region,

(iii) Escaping region Σ_E: $\langle F_1(Z), H_Z(Z)\rangle < 0$ and $\langle F_2(Z), H_Z(Z)\rangle > 0$ hold true, which suggests that trajectories on Σ_E will move towards either S_1 or S_2,

where $\langle \cdot, \cdot \rangle$ represents the standard scalar product and the non-vanishing gradient of H(Z) is expressed by $H_Z(Z)$. However, note that the escaping region is impossible in this paper as $\langle F_1(Z), H_Z(Z)\rangle < 0$ and $\langle F_2(Z), H_Z(Z)\rangle > 0$ cannot hold simultaneously.

In order to investigate the sliding mode dynamics for Filippov system(2.3), we need to know exactly about the sliding domain on Σ, so the renowned Filippov's convex method [25] and Utkin's equivalent control method [26] are both feasible. Let

$$\sigma(Z) = \langle F_1(Z), H_Z(Z)\rangle \langle F_2(Z), H_Z(Z)\rangle,$$

then the sliding mode domain can be determined by $\{Z \in D | \sigma(Z) < 0\}$ due to the absence of the escaping region.

Next, the definitions of several types of equilibria for system(2.3) are introduced.

Definition 2.1. For one point E_R, if it satisfies $F_i(E_R) = 0$ and locates on the corresponding region S_i, i=1,2, it is a real equilibrium for system(2.3).

Definition 2.2. If the point E_V is satisfied with the equation $F_i(E_V) = 0$ but located in another region S_j, i,j=1,2, i$\neq$ j, it is a virtual equilibrium for system(2.3).

Definition 2.3. If an equilibrium E_p is on the sliding mode Σ_S of system(2.3), that is, the equation $\lambda F_1(E_p) + (1-\lambda)F_2(E_p) = 0$ and $H(E_p) = 0$ hold true, where $0 < \lambda < 1$ and

$$\lambda = \frac{\langle H_Z(E_p),\ F_2(E_p)\rangle}{\langle H_Z(E_p),\ F_2(E_p) - F_1(E_p)\rangle},$$

it is a pseudo-equilibrium for system(2.3).

Definition 2.4. If a point E_b is an equilibrium of any subsystem(F_1 or F_2) but belongs to the separating boundary Σ, it is called a boundary equilibrium. In other words, a boundary equilibrium E_b satisfies $F_1(E_b) = 0$ or $F_2(E_b) = 0$ under the condition of $H(E_b) = 0$.

Definition 2.5. A tangency equilibrium E_T of system(2.3) is the one which belongs to the separating boundary Σ, i.e., $H(E_T) = 0$ and satisfies $\langle H_Z(E_T),\ F_1(E_T)\rangle \langle H_Z(E_T),\ F_2(E_T)\rangle = 0$.

For the subsystem F_1, since Huang [24] has analyzed this class of models, we only present main results from that paper here. This model has an equilibrium $E_{10} = (K, 0)$, which is a saddle and unstable all the time, and an unique positive equilibrium $E_1 = \left(\frac{rhK}{mK + rh}, \frac{rh}{mK + rh}\right)$, which is locally aymptotically stable.

And in region S_2, the subsystem F_2 exists two equilibria as well, $E_{20} = \left(K\left(1 - \frac{p_1}{r}\right), 0\right)$, and an unique internal equilibrium $E_2 = \left(\frac{shK(r-p_1)}{hrs + mK(s+p_2)}, \frac{K(r-p_1)(s+p_2)}{hrs + mK(s+p_2)}\right)$.

Lemma 2.1. *Suppose that $Z(t) = (x(t), y(t))^T$, $x(t) > 0$, $y(t) \geq 0$, is a solution of system(2.3) with the initial value $Z_0 = (x(t_0), y(t_0))^T$, $x(t_0) > 0$, $y(t_0) \geq 0$, then $Z(t)$ is always positive on $t \in [0, T)$.*

Proof. For the function f_1, we can get

$$\left.\frac{dx}{dt}\right|_{x\to 0} = \left[rx\left(1 - \frac{x}{K}\right) - mxy - \gamma p_1 x\right]_{x\to 0} = 0,$$

and for another function f_2, we have

$$\left.\frac{dy}{dt}\right|_{y=0} = \left[sy\left(1 - \frac{hy}{x}\right) + \gamma p_2 y\right]_{y=0} = 0.$$

Therefore, $Z(t)$ is positive for all $t \in [0, T)$ as long as the initial solution satisfying $x(0) > 0$ and $y(0) > 0$.

Lemma 2.2. *Denote the set $D = \{(x, y) \in R^2 | x > 0, y \geq 0\}$, and the set $\Omega = \left\{(x, y) \in D \middle| x \leq K,\ y \leq \frac{(s+p_2)K}{h}\right\}$ is positively invariant and attracting for model(2.3) with*

any given original values in D.

Proof. For the first function in system(2.1), we have

$$\frac{dx}{dt} = x\left(r - \frac{rx}{K} - my - \gamma p_1\right) \le x\left(r - \frac{rx}{K}\right), \tag{6}$$

which means that $\frac{dx}{dt} \le 0$ as long as $x = K$. And from the above equation, we can get

$$x(t) \le \frac{K}{1 + cKe^{-rt}},$$

which results in

$$\lim_{t\to+\infty} x(t) \le K.$$

Similarly, combining the above result, for the second function f_2 in system(2.1), we can obtain

$$\frac{dy}{dt} = y\left(s + \gamma p_2 - \frac{shy}{x}\right) \le y\left(s + p_2 - \frac{shy}{K}\right), \tag{7}$$

thus $\frac{dy}{dt} \le 0$ if $y = 0$ or $y = \frac{(s+p_2)K}{sh}$. And from equation(2.5), we have

$$y(t) \le \frac{(s+p_2)K}{sh + cK(s+p_2)e^{-(s+p_2)t}},$$

which means that $\lim_{t\to+\infty} y(t) \le \frac{(s+p_2)K}{sh}$. Obviously, $\{y \mid y(t) \le 0\} \subseteq \left\{y \,\middle|\, y(t) \le \frac{(s+p_2)K}{sh}\right\}$. Therefore, Ω is a positively invariant set and is attracting likewise.

Theorem 2.1. *The equilibrium E_1 is globally asymptotically stable in region S_1.*

Proof. Here we choose a Dulac function $B(x,y) = \frac{1}{xy}$, we have

$$\frac{\partial(Bf_{11})}{\partial x} + \frac{\partial(Bf_{12})}{\partial y} = -\frac{r}{Ky} - \frac{hs}{x^2} \le 0.$$

Therefore, by the Bendixson-Dulac criterion, there are no limit cycles in region S_1. Based on the local stability of E_1, hence E_1 is a globally asymptotically stable equilibrium.

Before analyzing properties of system(2.3), we give some assumptions as follows:

$$(H_1) \quad \frac{2hrs}{K(s+p_2)(r-p_1)} < 1,$$
$$(H_2) \quad \frac{2hrs}{K(s+p_2)(r-p_1)} > 1.$$

Lemma 2.3 *There are no closed orbits existing in region S_2.*

Proof. We use the same Dulac function $B(x,y) = \frac{1}{xy}$, and here we can get

$$\frac{\partial(Bf_{21})}{\partial x} + \frac{\partial(Bf_{22})}{\partial y} = -\frac{r}{Ky} - \frac{hs}{x^2} \le 0.$$

Thus, according to the Bendixson-Dulac criterion, there are not any closed orbits in region S_2.

Theorem 2.2. *When (H_1) holds, the equilibrium E_{20} is a saddle, which is always unstable. Otherwise, if (H_2) holds, E_{20} is globally asymptotically stable.*

Proof. Consider the Jacobian matrix of system(2.3) at E_{20}:

$$J(E_{20}) = \begin{pmatrix} p_1 - r & -mK\left(1 - \frac{p_1}{r}\right) \\ 0 & s + p_2 - \frac{2hrs}{K(r-p_1)} \end{pmatrix},$$

then we can get eigenvalues straightforward:

$$\lambda_1 = p_1 - r \;\; and \;\; \lambda_2 = s + p_2 - \frac{2hrs}{K(r-p_1)},$$

where $\lambda_1 < 0$ as $r > p_1$.

Therefore, if $\lambda_2 > 0$, two eigenvalues have opposite signs, that is, E_{20} is a saddle. And if $\lambda_2 < 0$, both eigenvalues are negative, so E_{20} is globally asymptotically stable based on the Lemma 2.3.

Theorem 2.3. *The internal equilibrium E_2 is globally asymptotically stable in region S_2.*

Proof. For simplicity, we denote that $q = hrs + mK(s+p_2)$, $q_1 = hsK(r-p_1)$, $q_2 = K(r-p_1)(s+p_2)$ in the first place, then we have $E_2 = \left(\frac{q_1}{q}, \frac{q_2}{q}\right)$. By calculation, the Jacobian matrix of system(2.3) is obtained as follows:

$$J(E_2) = \begin{pmatrix} r - \frac{2rq_1}{Kq} - \frac{mq_2}{q} - p_1 & -\frac{mq_1}{q} \\ hs\frac{{q_2}^2}{{q_1}^2} & s + p_2 - \frac{2hsq}{q_1)} \end{pmatrix},$$

from which we get the characteristic equation

$$\lambda^2 + B\lambda + C = 0,$$

where,

$$B = \frac{2r{q_1}^2 + mKq_1q_2 - 2hsKq^2}{Kqq_1} - (r-p_1) - (s+p_2),$$

$$C=\frac{hmsq_2{}^2}{qq_1}+\left(r-\frac{rq_1}{Kq}-\frac{mq_2}{q}-p_1\right)\left(s-\frac{2hsq_2}{q_1}+p_2\right).$$

Let $C_1=\dfrac{hmsq_2{}^2}{qq_1}$,

$C_2=\left(r-\dfrac{rq_1}{Kq}-\dfrac{mq_2}{q}-p_1\right)\left(s-\dfrac{2hsq_2}{q_1}+p_2\right)$,

so $C=C_1+C_2$.

Notice that $B>0$ when

$$\frac{rq_1{}^2+mKq_1q_2+2hsKqq_2}{qq_1K\left[(r-p_1)+(s+p_2)\right]}>1.$$

So here we substitute values of $q,q_i,i=1,2$, into the left-hand side of the above inequality and simplify it:

$$\begin{aligned}1<&\frac{rh^2s^2K^2(r-p_1)^2+hmsK^3(s+p_2)(r-p_1)^2}{K\left[hsK(r-p_1)\right]\left[hsK+mK(s+p_2)\right]\left[(r-p_1)+(s+p_2)\right]}\\&+\frac{+2hsK^2(r-p_1)(s+p_2)\left[hrs+mK(s+p_2)\right]}{K\left[hsK(r-p_1)\right]\left[hsK+mK(s+p_2)\right]\left[(r-p_1)+(s+p_2)\right]}\\=&\frac{\left[hsK^2(r-p_1)\right]\left[hrs+mK(s+p_2)\right]\left[(r-p_1)+2(s+p_2)\right]}{\left[hsK^2(r-p_1)\right]\left[hrs+mK(s+p_2)\right]\left[(r-p_1)+(s+p_2)\right]}\\=&\frac{(r-p_1)+2(s+p_2)}{(r-p_1)+(s+p_2)}.\end{aligned}$$

Obviously this inequality holds, that is, $B>0$ is true.

Similarly, substitute values of $q,q_i,i=1,2$, into the formula of C:

$$\begin{aligned}C_1&=\frac{hmsq_2{}^2}{qq_1}=\frac{hmsK^2(r-p_1)^2(s+p_2)^2}{hsK(r-p_1)\left[hrs+mK(s+p_2)\right]}>0,\\C_2&=\left(r-\frac{rq_1}{Kq}-\frac{mq_2}{q}-p_1\right)\left(s-\frac{2hsq_2}{q_1}+p_2\right)\\&=\left\{(r-p_1)-\frac{hrsK(r-p_1)+mK^2(r-p_1)(s+p_2)}{K\left[hrs+mK(s+p_2)\right]}\right\}\left[-(s+p_2)\right]\\&=0,\end{aligned}$$

which means that $C>0$ is established.

Hence, according to Routh-Hurwitz criteria, the internal equilibrium E_2 is locally asymptotically stable, and combined with Lemma 2.3, E_2 is globally asymptotically stable in region S_2.

3 Dynamics of sliding mode and equilibria

In this section, we initially pay attention to the existence of the sliding domain, and then we study sliding mode dynamics. In the end, different types of equilibria are discussed.

In view of preliminaries, the sliding mode are defined as

$$\Sigma_S=\{Z\in\Sigma\,|\sigma(Z)<0\},$$

where

$$\begin{aligned}\sigma(Z)&=f_{11}\cdot f_{21}\\&=\left[rx\left(1-\frac{x}{K}\right)-mxy\right]\cdot\left[rx\left(1-\frac{x}{K}\right)-mxy-p_1x\right].\end{aligned}$$

As a result, $\sigma(Z)<0$ is equivalent to

$$rx\left(1-\frac{x}{K}\right)-mxy>0\quad and\quad rx\left(1-\frac{x}{K}\right)-mxy-p_1x<0.$$

By calculation, we get

$$y_{min}<y<y_{max},$$

and

$$y_{min}=\frac{r}{m}\left(1-\frac{ET}{K}\right)-\frac{p_1}{m},\quad y_{max}=\frac{r}{m}\left(1-\frac{ET}{K}\right).$$

Hence the sliding segment of Filippov system(2.3) can be expressed by

$$\Sigma_S=\left\{(x,y)\in D\;\middle|\;x=ET,\quad y_{min}<y<y_{max}\right\}.$$

Note. There is no escaping region for Filippov system(2.3), as it is impossible that the two inequalities $\langle H_Z(Z),F_{S_1}(Z)\rangle<0$ and $\langle H_Z(Z),F_{S_2}(Z)\rangle>0$ are satisfied in the meantime.

Now, we use Utkin's equivalent control method [26] to probe for the dynamics of the sliding segment.

In light of this method, we can obtain the differential equation for sliding dynamics on the segment Σ_S. It follows from $H=0$ and the first equation of Filippov system(2.3) that

$$\frac{dH}{dt}=\frac{dx}{dt}=rx\left(1-\frac{x}{K}\right)-mxy-\gamma p_1x=0.$$

Solving the above equation respect to γ produces

$$\gamma=\frac{r}{p_1}\left(1-\frac{x}{K}\right)-\frac{m}{p_1}y.$$

Substituting the formula of γ into the second equation in model(2.1) generates

$$\frac{dy}{dt}=\left[s\left(1-\frac{h}{x}y\right)\right]y+\frac{rp_2}{p_1}\left(1-\frac{x}{K}\right)y-\frac{mp_2}{p_1}y^2\doteq\psi(y),$$

which determines the dynamics on Σ_S.

The following is to explore different kinds of equilibria. Based on the analysis of section 2, there is an unique positive equilibrium in each subsystem, that is, $E_1=\left(\frac{rhK}{mK+rh},\frac{rh}{mK+rh}\right)$ in S_1 and $E_2=\left(\frac{shK(r-p_1)}{hrs+mK(s+p_2)},\frac{K(r-p_1)(s+p_2)}{hrs+mK(s+p_2)}\right)$ in S_2. The discussion of these two equilibria types is shown below:

(i) Since $\frac{hrK}{mK+hr} > \frac{hsK(r-p_1)}{hrs+mK(s+p_2)}$, it is unlikely that $\frac{hrK}{mK+hr} < ET < \frac{hsK(r-p_1)}{hrs+mK(s+p_2)}$ holds. In other words, E_1 and E_2 cannot become real equilibria simultaneously.

(ii) When $\frac{hrK}{mK+hr} < ET$, E_1 is a real equilibrium denoted by E_R^1, while E_2 is a virtual equilibrium as $\frac{hsK(r-p_1)}{hrs+mK(s+p_2)} < ET$, denoted by E_V^2.

(iii) If $\frac{hsK(r-p_1)}{hrs+mK(s+p_2)} > ET$, E_2 is a real equilibrium denoted by E_R^2, and E_1 is a virtual equilibrium expressed by E_V^1.

(iv) Due to the fact that $\frac{hsK(r-p_1)}{hrs+mK(s+p_2)} < ET < \frac{hrK}{mK+hr}$ is true, in this case, both equilibria are virtual recorded as E_V^1, E_V^2.

Now, we probe for the pseudo-equilibrium. Solving the equation $\psi(y) = 0$ yields

$$y_1 = 0 \ \ and \ \ y_2 = \frac{r\left(1-\frac{ET}{K}\right)+\frac{sp_1}{p_2}}{m+\frac{hsp_1}{p_2 ET}}.$$

As $y_1 < y_{min}$, we omit this solution. In order to make sure that $y_2 \in (y_{min}, y_{max})$, it must have:

$$\frac{r}{m}\left(1-\frac{ET}{K}\right)-\frac{p_1}{m} < \frac{r\left(1-\frac{ET}{K}\right)+\frac{sp_1}{p_2}}{m+\frac{hsp_1}{p_2 ET}} < \frac{r}{m}\left(1-\frac{ET}{K}\right),$$

during which we can obtain

$$\frac{hsK(r-p_1)}{hrs+mK(s+p_2)} < ET < \frac{hrK}{mK+hr},$$

where both of internal equilibria happen to exist as two virtual equilibria E_V^1, E_V^2. Therefore, the pseudo-equilibrium $E_p = (ET, y_2)$ cannot coexist with any regular equilibrium.

According to definition 2.4, the boundary equilibria satisfy $x = ET$ and equations:

$$\begin{cases} \dfrac{dx(t)}{dt} = rx\left(1-\dfrac{x}{K}\right) - mxy = 0, \\ \dfrac{dy(t)}{dt} = y\left[s\left(1-\dfrac{h}{x}y\right)\right] = 0, \end{cases}$$

or

$$\begin{cases} \dfrac{dx(t)}{dt} = rx\left(1-\dfrac{x}{K}\right) - mxy - p_1 x = 0, \\ \dfrac{dy(t)}{dt} = y\left[s\left(1-\dfrac{h}{x}y\right)\right] + p_2 y = 0. \end{cases}$$

Hence we can get two boundary equilibria below:

$$E_B^1 = \left(ET, \frac{ET}{h}\right), \ \ where \ \ ET = \frac{hrK}{hr+mK},$$

and

$$E_B^2 = \left(ET, \frac{(s+p_2)ET}{hs}\right), \ \ where \ \ ET = \frac{hsK(r-p_1)}{hrs+mK(s+p_2)}.$$

Correspondingly, tangent points satisfy $x = ET$ and equations:

$$rx\left(1-\frac{x}{K}\right) - mxy = 0 \ \ or \ \ rx\left(1-\frac{x}{K}\right) - mxy - p_1 x = 0,$$

so we get two tangent points as shown below:

$$E_T^1 = \left(ET, \frac{r}{m}\left(1-\frac{ET}{K}\right)\right)$$

and

$$E_T^2 = \left(ET, \frac{r\left(1-\frac{ET}{K}\right)-p_1}{m}\right),$$

which are endpoints of sliding segment Σ_S.

Lemma 3.1. *The pseudo-equilibrium E_p is locally asymptotically stable respect to Σ_S.*

Proof. For the dynamic equation of Σ_S, namely $\psi(y)$, we can take the derivative with regard to y at E_p:

$$\psi'(E_p) = -\frac{sp_1 K + rp_2(K-ET)}{p_1 K} < 0.$$

Therefore, on the basis of stability theory for ODEs, E_p is locally asymptotically stable on Σ_S.

4 Global dynamics and numerical simulation

In this section, we concentrate on the global dynamical behaviors that the Filippov system(2.3) can exhibit. Initially, we rule out the existence of three kinds of possible limit cycles, and then with combining properties of equilibria, the global stability of equilibria can be obtained.

According to the analysis in section 2, we can make sure that there is no limit cycle totally contained within the region S_1 and S_2. Then we have the following lemmas.

Lemma 4.1. *There is no closed orbit completely contained within the region S_i(i=1,2).*

Next, we give proofs of non-existence of the other limit cycles which respectively contain a part of the sliding

segment and the entire sliding mode.

Lemma 4.2. *There exists no closed orbit which contains partial sliding domain.*

Proof. We prove it by reduction to absurdity. There are two cases in all, namely, the pseudo-equilibrium E_p exists or not. So when E_p exists on the sliding segment, it is stable such that all solutions nearby will converge to this point finally. However, suppose that there is a limit cycle including part of the sliding domain, some trajectories that once touch the sliding domain converge to this limit cycle, which contradicts the stability of the pseudo-equilibrium.

On the other hand, when E_p does not exist, there are a real equilibrium and a virtual equilibrium coexisting in a certain region. Without loss of generality, assume that this kind of limit cycle denoted by L contains a real equilibrium E_1 in the region S_1. This means that any trajectory outside L will converge to itself and cannot reach E_1 anymore, which contradicts the global stability of the real equilibrium E_1 in the region S_1. Hence, there does not exist any closed orbit including part of the sliding domain.

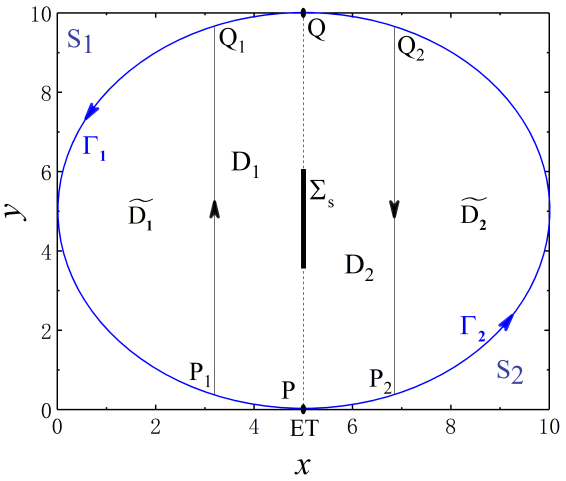

Fig. 1 The schematic of the possible limit cycle which surrounds the sliding segment.

Lemma 4.3. *There does not exist a closed orbit surrounding the entire sliding domain.*

Proof. Suppose that there is a closed orbit $\Gamma = \Gamma_1 + \Gamma_2$ around the sliding segment (shown as Fig1), where $\Gamma_i = \Gamma \bigcap S_i,\ i = 1, 2$. And Γ intersects with the switching line $x = ET$ at points P and Q. Denote the region enclosed by Γ as D and $D_i = D \bigcap S_1,\ i = 1, 2$. Then we have two auxiliary lines $x = ET - \theta$ and $x = ET + \theta$, which intersect with Γ at points P_1, Q_1 and P_2, Q_2 respectively. Meanwhile, $P_1 = P - a_1(\theta)$, $Q_1 = Q - b_1(\theta)$, $P_2 = P + a_2(\theta)$, $Q_2 = Q + b_2(\theta)$, where $a_i(\theta)$ and $b_i(\theta)$ $(i = 1, 2)$ are continuous with respect to θ and $\lim\limits_{\theta\to 0} a_i(\theta) = \lim\limits_{\theta\to 0} b_i(\theta) = 0,\ i = 1, 2$. This means that P_1Q_1 and P_2Q_2 tends to PQ with $\theta \to 0$. Moreover, describe two regions delimited by Γ_1, P_1Q_1 and Γ_2, P_2Q_2 as $\widetilde{D_1}$ and $\widetilde{D_2}$ respectively, which severally tend to D_1 and D_2 when $\theta \to 0$.

Let the Dulac function be $B = \dfrac{1}{xy}$, then we can obtain the following results by using Green's theorem.

After the above analysis, it is easy to get that

$$\sum_{i=1}^{2} \iint_{D_i} \left[\frac{\partial(Bf_{i1})}{\partial x} + \frac{\partial(Bf_{i2})}{\partial y}\right] dx\,dy$$

$$= \lim_{\theta\to 0} \sum_{i=1}^{2} \iint_{\widetilde{D_i}} \left[\frac{\partial(Bf_{i1})}{\partial x} + \frac{\partial(Bf_{i2})}{\partial y}\right] dx\,dy$$

$$= \alpha,$$

that is, we denote the result of the above equation by α.

By calculations, we have

$$\sum_{i=1}^{2} \left[\frac{\partial(Bf_{i1})}{\partial x} + \frac{\partial(Bf_{i2})}{\partial y}\right] = -\frac{2r}{Ky} - \frac{2hs}{x^2} < 0,$$

which means that $\alpha < 0$ is right.

Then, according to Green's theorem, we have:

$$\iint_{\widetilde{D_1}} \left[\frac{\partial(Bf_{11})}{\partial x} + \frac{\partial(Bf_{12})}{\partial y}\right] dx\,dy$$

$$= \oint_{\widehat{Q_1\Gamma_1P_1} + \overrightarrow{P_1Q_1}} (Bf_{11})dy - (Bf_{12})dx$$

$$= \int_{\Gamma_1} (Bf_{11})dy - (Bf_{12})dx \ + \ \int_{P_1}^{Q_1} (Bf_{11})dy - (Bf_{12})dx$$

$$= \int_{P_1}^{Q_1} (Bf_{11})dy.$$

Notice that along Γ_1, we have $dy = f_{12}dt$, $dx = f_{11}dt$, and along $\overrightarrow{P_1Q_1}$, we have $dx = 0$.

Similarly, we have

$$\iint_{\widetilde{D_2}} \left[\frac{\partial(Bf_{21})}{\partial x} + \frac{\partial(Bf_{22})}{\partial y}\right] dx\,dy = \int_{P_2}^{Q_2} (Bf_{21})dy.$$

Therefore,

$$\alpha = \lim_{\theta\to 0} \left[\int_{P_1}^{Q_1} (Bf_{11})dy + \int_{P_2}^{Q_2} (Bf_{21})dy\right]$$

$$= \int_{P}^{Q} \frac{p_1}{y}\, dy$$

$$= p_1 \ln\left(\frac{Q}{P}\right) > 0,$$

as Q is greater than P along the vertical axis.

This causes a contradiction. Hence we can obtain the conclusion as Lemma 4.3.

In what follows, we investigate the global dynamics of Filippov system(2.3), and then the global stability of internal equilibria and pseudo-equilibrium is obtained with the support of numerical simulation.

Theorem 4.1. *The pseudo-equilibrium E_p is globally asymptotically stable as long as it exists.*

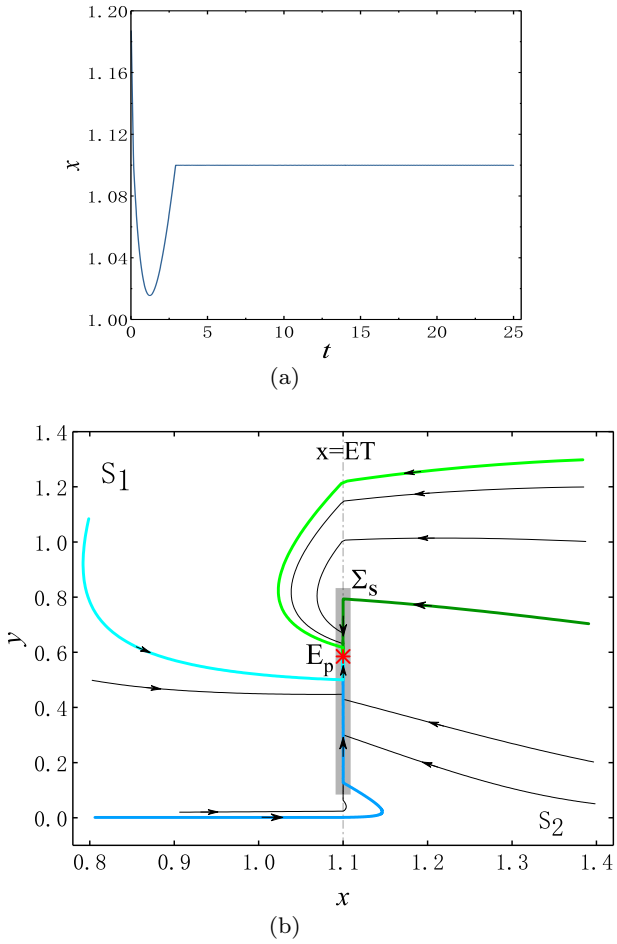

Fig. 2 (a): Time history diagram of Filippov system(2.3) when the pseudo-equilibrium E_p exists, which shows that trajectories are prone to be stable finally. (b): The phase portrait of Filippov system(2.3) when $\frac{hsK(r-p_1)}{hrs+mK(s+p_2)} < ET < \frac{hrK}{mK+hr}$, which exhibits the global asymptotically stability of pseudo-equilibrium E_p. The other fixed parameters are set as: $r = 0.5, K = 3, m = 0.4, s = 0.3, h = 2.4, q_1 = 0.3, q_2 = 0.3$, and ET=1.1.

Proof. From the analysis in section 3, we know that two internal equilibria E_1, E_2 are both virtual denoted as E_V^1 and E_V^2 when E_p exists. This implies that the internal equilibrium E_1 belonging to the region S_1 is in the region S_2, and E_2 is an internal equilibrium of the region S_2 but is in the region S_1. Therefore, all trajectories move towards the opposite domain to reach their own equilibrium and they are bound to touch the switching line x=ET. Since E_p is LAS on the sliding segment and there does not exist any limit cycle in terms of Lemmas 4.1-4.3, some trajectories which hit the sliding mode Σ_S in the switching line will slide to E_p, while other trajectories which pass through the switching line to the opposite area will return and ultimately approach to E_p after colliding with the sliding segment. So it follows that E_p is globally asymptotically stable when it is present. The result of numerical simulation is shown in the figure below.

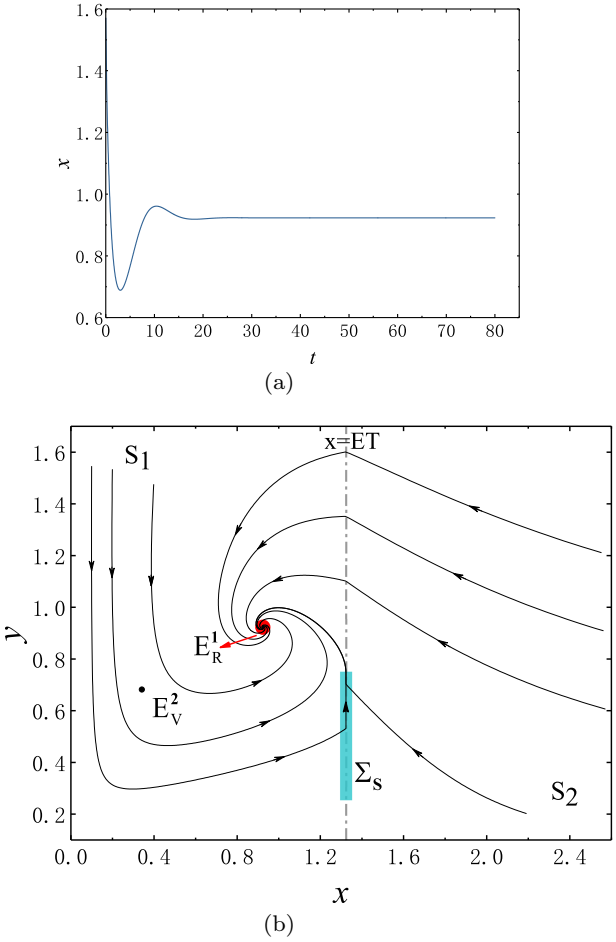

Fig. 3 (a): Time history diagram of system(2.3) when $\frac{hrK}{mK+hr} < ET$ is true, which shows the stability of E_1. (b): The phase portrait of system(2.3) when E_1 is the only real equilibrium, which indicates that all solutions tend to E_1 eventually. The fixed parameters are given as follows:$r = 0.8, K = 3, m = 0.6, s = 0.3, h = 1, q_1 = 0.3, q_2 = 0.3$, and ET=1.3231.

Theorem 4.2. *The internal equilibrium E_1 is globally asymptotically stable for the Filippov system(2.3) if $\frac{hrK}{mK+hr} < ET$.*

Proof. In the light of the discussion in section 3, when $\frac{hrK}{mK+hr} < ET$, E_p does not exist, and E_1 is a real equilibrium expressed by E_R^1 located in the region S_1 and E_2 is a virtual equilibrium described as E_V^2 situated at the region S_1 as well. Meanwhile, on the basis of Theorem 2.1, E_1 is GAS in the region S_1, and there is no closed orbit for this Filippov system(2.3) by Lemmas 4.1-4.3.

Consequently, as Fig 3 shows, trajectories starting from the region S_1 will either approach to E_R^1 straightforward or intersect with the sliding segment Σ_S on the switching line and slide to the top endpoint along this segment, then get into the region S_1 again to reach E_R^1. On the other hand, trajectories whose initial points are in the region S_2 will firstly move towards S_1 to reach their own equilibrium E_2. Hence these trajectories will either pass through the switching line to S_1 and go towards E_R^1 or collide with Σ_S and slide up to the end, then approach to E_R^1 in the region S_1. In view of this, all trajectories will reach E_R^1 ultimately, that is, E_R^1 is GAS for system(2.3).

Theorem 4.3. *If $\frac{hsK(r-p_1)}{hrs+mK(s+p_2)} > ET$ holds, the internal equilibrium E_2 is globally asymptotically stable for the Filippov system(2.3).*

Proof. Combining the analysis in section 3, we have that when $\frac{hsK(r-p_1)}{hrs+mK(s+p_2)} > ET$ holds, there are two equilibria in total, namely, E_R^2 and E_V^1 both in the region S_2. Moreover, according to Theorem 2.3, E_2 is GAS in the region S_2, and no closed orbit exists for system(2.3) by Lemmas 4.1-4.3.

Thus, as Fig 4 shows, trajectories initiating from the region S_2 will tend to E_R^2 directly, or once they hit the sliding segment, they will swipe down along this segment to the endpoint and then enter the region S_2 to reach E_R^2. Furthermore, trajectories starting from the region S_1 are attracted by E_1 in the opposite region. So they will either go across the switching line and move towards E_R^2 or collide with the sliding segment and slide down to approach to E_R^2 in the region S_2. It then follows that all solutions will converge to E_R^2 finally, in other words, E_R^2 is a GAS node for the system(2.3).

Finally, we find that the parameter ET plays an important role in the pest control. Denote $\frac{rhK}{mK+rh}$ and $\frac{hsK(r-p_1)}{hrs+mK(s+p_2)}$ as A and B respectively, and $A > B$ holds based on the analysis in section 3. By employing numerical simulation, the tendency of solutions with different

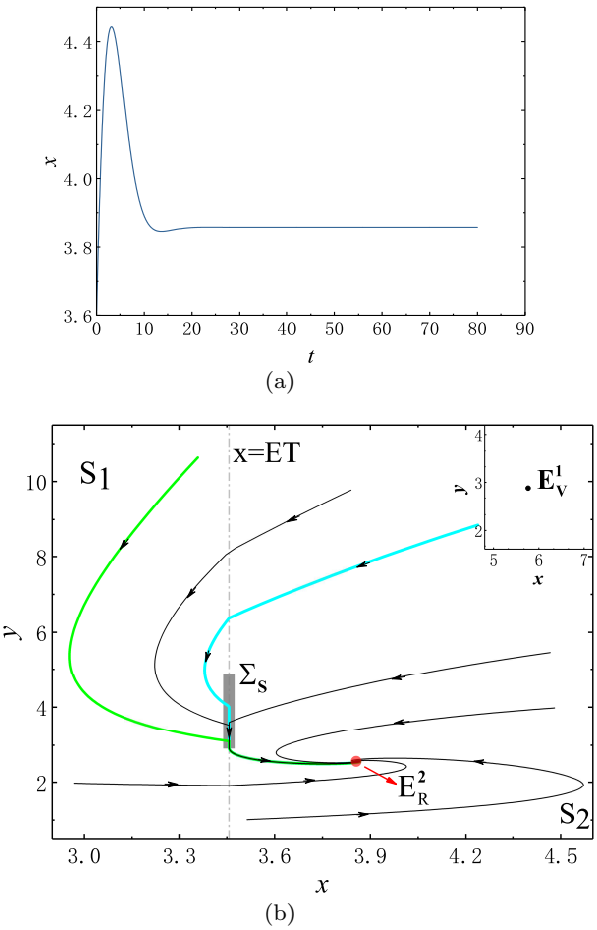

Fig. 4 (a): Time history diagram of system (2.3) when $\frac{hsK(r-p_1)}{hrs+mK(s+p_2)} > ET$ holds, which shows that E_2 is indeed stable finally. (b): The phase portrait of system(2.3) when equilibrium E_2 is the only real one, which clearly shows the global dynamics of system(2.3) in this situation. The fixed parameters are:$r = 0.8, K = 9, m = 0.1, s = 0.3, h = 2, q_1 = 0.2, q_2 = 0.1$, and ET=3.4571.

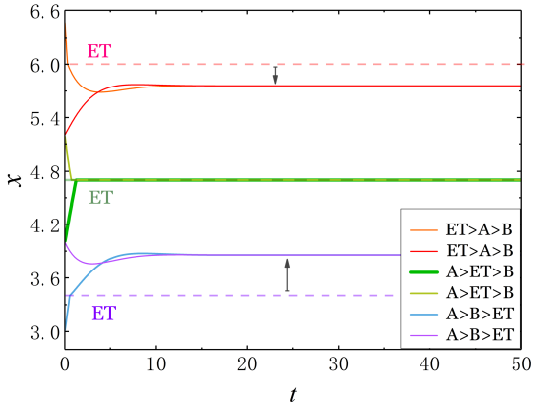

Fig. 5 Solutions of Filippov system(2.3) with various ET, where the values of fixed parameters are $r = 0.8, K = 9, m = 0.1, s = 0.3, h = 2, q_1 = 0.2, q_2 = 0.1$. It demonstrates that ET should be greater than $\frac{hsK(r-p_1)}{hrs+mK(s+p_2)}$.

ET are exhibited in Fig 5. We can see clearly that only if $ET > B$ holds, all trajectories would approach to either the pseudo-equilibrium on the switching line Σ or the internal equilibrium in the region S_1, which implies that the pest population is controlled and eventually stabilize at or below ET, in other words, our control tactics work.

5 Biological implications and conclusions

Nowadays, the Filippov system has been found to be useful to describe the real-world problems and investigated in many fields[27–29]. Compared with the impulsive differential equations, the non-smooth Filippov system is more close to the reality in describing pest control measures. And despite many papers have studied Leslie-Gower model, none of them have considered the effect of control strategies. Hence we expand the LG model with Holling I functional response into a piecewise smooth system by applying IPM strategies, which can be called as a Filippov system with the threshold policy as well. This means that we do not take any action when the number of pests is below the economic threshold(ET), but in case the quantity reaches or exceeds ET, we will spray pesticides and release the natural enemy in the meantime. In order to minimize the economic toll and maximize the crop yield, our goal in this paper is to get the conditions under which the pest population can stabilize at or below the value given in advance. So we make use of Filippov theories and qualitative techniques with numerical simulations to investigate dynamical behaviors of proposed system in detail, including global dynamics of subsystems, the existence of sliding mode and different types of equilibria, sliding mode dynamics and the global stability of equilibria.

It is worth mentioning that no possible limit cycle exists for our proposed system and all trajectories are able to converge to the certain equilibrium finally under some conditions rather than exhibiting divergence or oscillation, which means that our strategies are feasible. Moreover, the results of global stability are concentrated in Theorems 4.1-4.3 and Figs 2-4. Especially, combining the outcome of numerical simulation in Fig 5, it is realized that the selection of ET plays a strong part in the pest control, as this offers the condition of choosing ET. Consequently, our findings are valuable for how to draw up strategies effectively and when to take measures.

References

1. Shabbir, A., Silva, R., Liu, S.S., Furlong, M.J., Zalucki, M.P.: Estimating the economic cost of one of the world's major insect pests, plutella xylostella (lepidoptera: Plutellidae): Just how long is a piece of string?. Journal Of Economic Entomology. (4), 4 (2012)
2. Zaman-Allah, M.A., Chaipa, I., Chari, N., Chinwada, P., Baudron, F.: Understanding the factors influencing fall armyworm (spodoptera frugiperda je smith) damage in african smallholder maize fields and quantifying its impact on yield. a case study in eastern zimbabwe. Crop Protection. 120, 141-150 (2019)
3. Ota, N., Hutchison, W.D., Beddow, J., Walsh, T., Tay, W.T., Borchert, D.M., Paula-Moreas, S.V., Czepak, C., Zalucki, M.P., Kriticos, D.J.: The potential distribution of invading helicoverpa armigera in north america: Is it just a matter of time. Plos One. 10(3), 24 (2015)
4. Turchen, L.M., Jumbo, L.O.V., Guedes, R.N.C., Pereira, E.J.G., Aguiar, R.W.S., Oliveira, E.E., Haddi, K.: Rethinking biorational insecticides for pest management: unintended effects and consequences. Pest Management Science. 76(7), 2286-2293 (2020)
5. Guo, J., Jiang, Y., Zhao, J., Sethi, A., He, K., Wang, Z., Jing, D.P.: Initial detections and spread of invasive spodoptera frugiperda in China and comparisons with other noctuid larvae in cornfields using molecular techniques. Insect Sci. 27(4), 780-790 (2020)
6. Reeves, P.T., Hoang, B.T., Mitter, N., Fletcher, S. J.: A perspective on rnai-based biopesticides. Frontiers In Plant Science. 11, 10 (2020)
7. Kumar, S., Datta, R., Lal, R., Vijayakumar, V., Brtnicky, M., Sharma, M.P., Yadav, G.S., Jhariya, M.K., Jangir, C.K., Pathan, S.I., Dokulilova, T., Pecina, V., Marfo, T.D., Meena, R.S.: Impact of agrochemicals on soil microbiota and management: A review. Land. 9(2), 21 (2020)
8. Li, Y., Wu, Y., Yang, Y.: Current status of insecticide resistance in helicoverpa armigera after 15 years of bt cotton planting in china. Journal of Economic Entomology. (1), 375-381 (2013)
9. Ghanim, M., Roditakis, E., Nauen, R., Ishaaya, I., Horowitz, A.R.: Insecticide resistance and its management in bemisia tabaci species. Journal of Pest Science. 93(3), 893-910 (2020)
10. F, Perveen.: Insecticides - advances in integrated pest management. All Journals. InTech (2012)

11. Mukerji, G., Ciancio, A.: Mycorrhizae In The Integrated Pest And Disease Management. General Concepts in Integrated Pest and Disease Management. 245-266 (2007)
12. Pedigo, L.P., Hutchins, S.H., Higley, L.: Economic injury levels in theory and practice. Annual Review of Entomology. 31, 341-368 (2003)
13. Kogan, M.: Integrated pest management: historical perspectives and contemporary developments. Annual Review of Entomology. 43(1), 243-270 (1998)
14. Hu, J., Yuen, P., Liu, J.: Extinction and permanence of the predator-prey system with general functional response and impulsive control. Applied Mathematical Modelling. 88, 55-67 (2020)
15. Tang, S., Cheke, R.A., Tian, Y.: Nonlinear state-dependent feedback control of a pest-natural enemy system. Nonlinear Dynamics. 94(3), 2243-2263 (2018)
16. Cheng, H., Li, Y., Zhang, X., Wang, J.: The geometrical analysis of a predator-prey model with multi-state dependent impulses. Journal Of Applied Analysis And Computation. 8(2), 427-442 (2018)
17. Tang, S., Zhang, X.: Existence of multiple sliding segments and bifurcation analysis of filippov prey–predator model. Applied Mathematics and Computation. 239, 265-284 (2014)
18. Xiao, Y., Zhang, Y.: Global dynamics for a filippov epidemic system with imperfect vaccination. Nonlinear Analysis: Hybrid Systems. 38, (2020)
19. Wang, L., Yang, Y.: Global dynamics and rich sliding motion in an avian-only filippov system in combating avian influenza. International Journal of Bifurcation and Chaos. 30(01), (2020).
20. Kang, Y.M., Smith, R., Chen, C.: Sliding motion and global dynamics of a filippov fire-blight model with economic thresholds. Nonlinear Analysis: Real World Applications. 39, 492-519 (2018)
21. Tan X., Tosato, M., Liu, X., Qin, W.: Threshold control strategy for a non-smooth filippov ecosystem with group defense. Applied Mathematics and Computation. 362, (2019)
22. Bhattacharyya, J., Roelke, D.L., Pal, S., Banerjee, S.: Sliding mode dynamics on a prey–predator system with intermittent harvesting policy. Nonlinear Dynamics. 98(2), 1299-1314 (2019)
23. Li, W., Ji, J., Huang, L., Wang, J.: Bifurcations and dynamics of a plant disease system under non-smooth control strategy. Nonlinear Dynamics. 99(4), 3351-3371 (2020)
24. Huang, Z.: Global stability for a class of predator-prey systems. Siam Journal on Applied Mathematics. 55(3), 763-783 (1995)
25. Filippov, A.F.: Differential equations with discontinuous righthand sides. Journal of Mathematical Analysis and Applications. 154(2), 99-128 (1999)
26. Utkin, V.I.: Sliding mode control design principles and applications to electric drives. IEEE Transactions on Industrial Electronics. 40(1), 23-36 (2002)
27. Cai, Z., Huang, J., Huang, L.: Periodic orbit analysis for the delayed filippov system. Proceedings Of the American Mathematical Society. 146(11), 4667-4682 (2018)
28. Duan, L., Fang, X., Huang, C.: Global exponential convergence in a delayed almost periodic nicholson's blowflies model with discontinuous harvesting. Mathematical Methods In the Applied Sciences. 41(5), 1954-1965 (2018)
29. Hu, C., Yu, J., Chen, Z., Jiang, H., Huang, T.: Fixed-time stability of dynamical systems and fixed-time synchronization of coupled discontinuous neural networks. Neural Networks. 89, 74-83 (2017)

Declaration

Funding Zhengdi Zhang has received research support from the National Natural Science Foundation of China(Grant No.11872189).

Conflict of interest We declare that we have no conflict of interest.

Data availability Data sharing is not applicable to this article as no datasets were generated or analysed during the current study.

Others are not applicable.

Figures

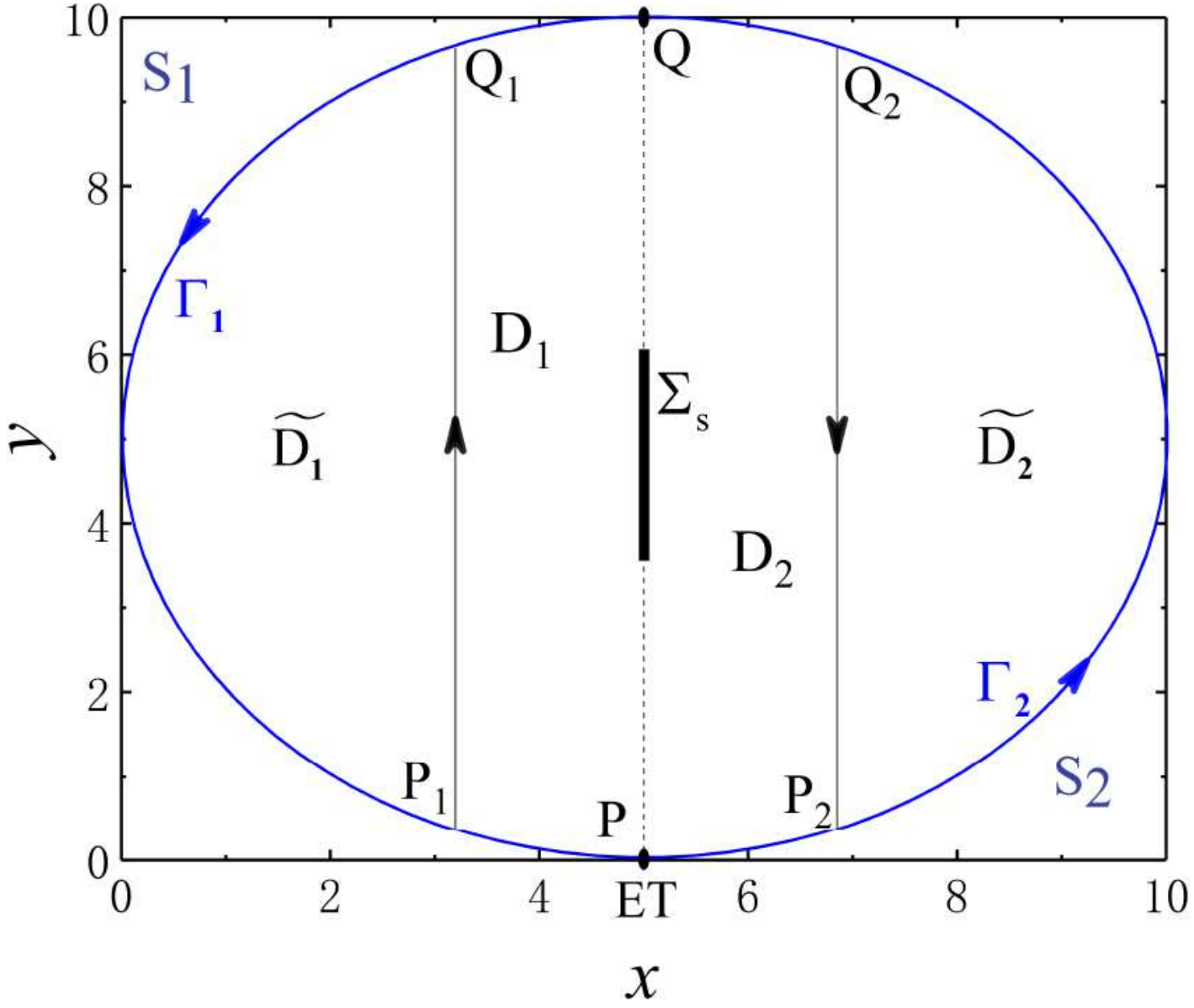

Figure 1

The schematic of the possible limit cycle which sur-rounds the sliding segment.

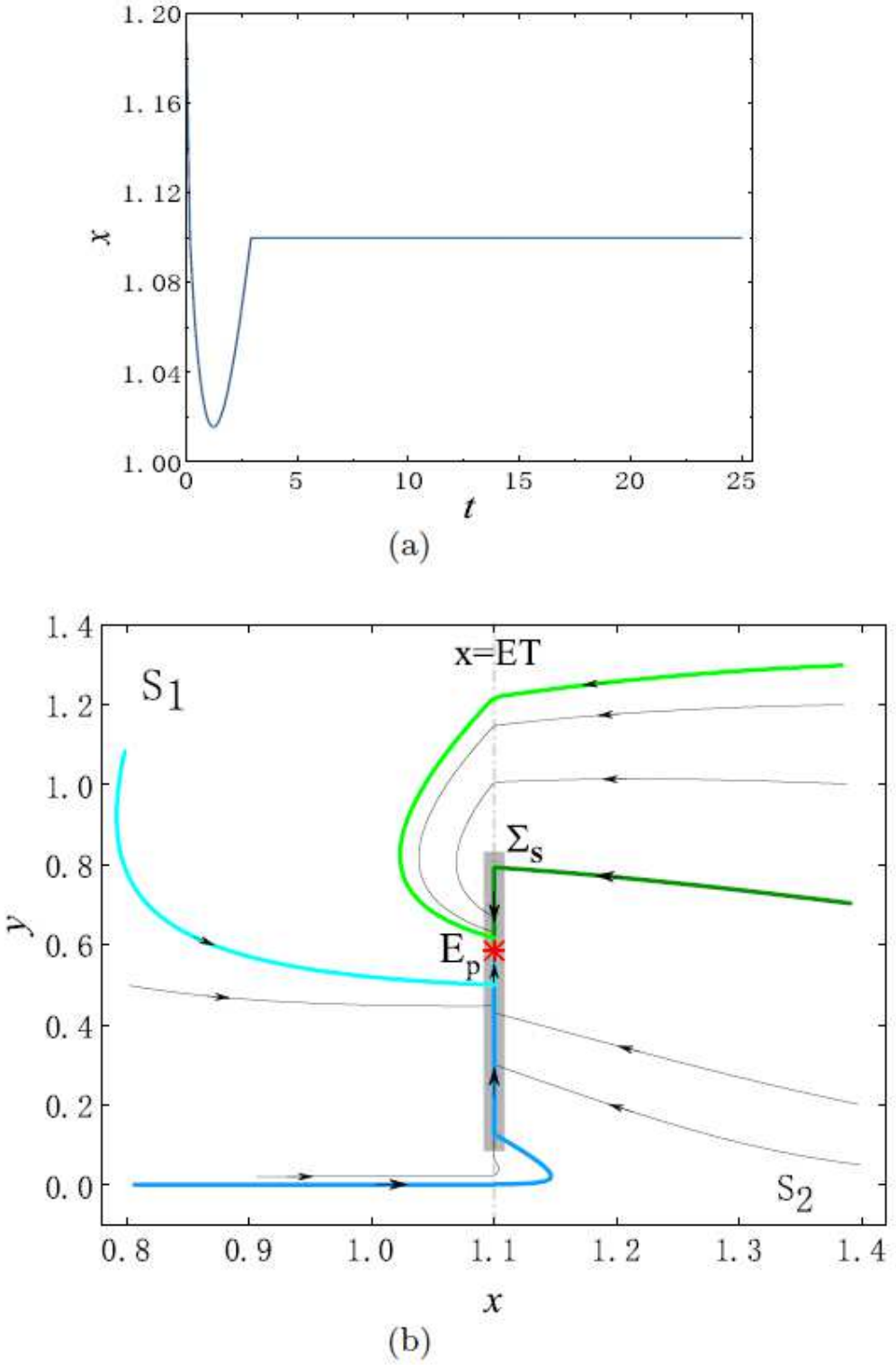

Figure 2

Please see manuscript .pdf for full caption.

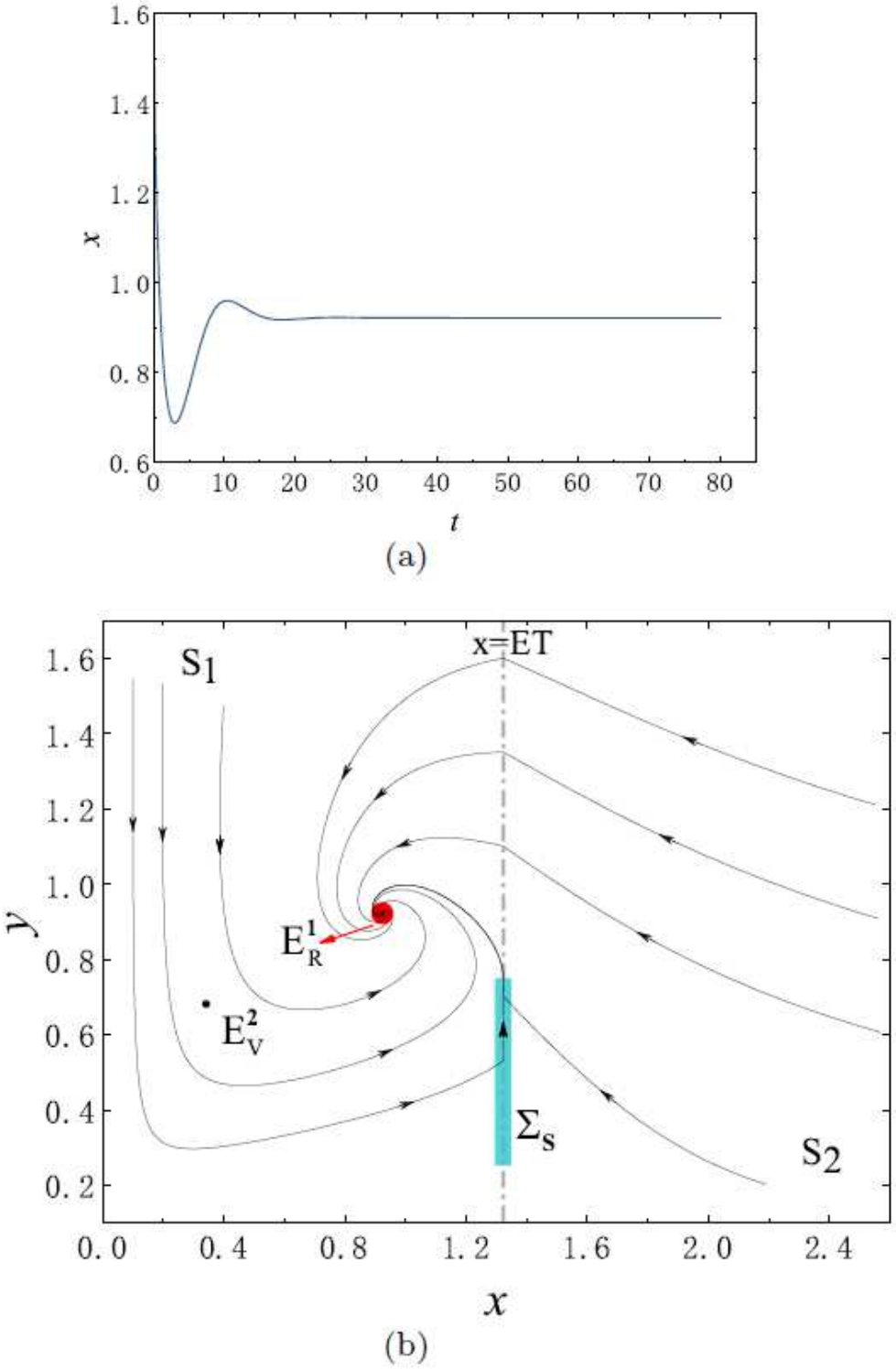

Figure 3

Please see manuscript .pdf for full caption.

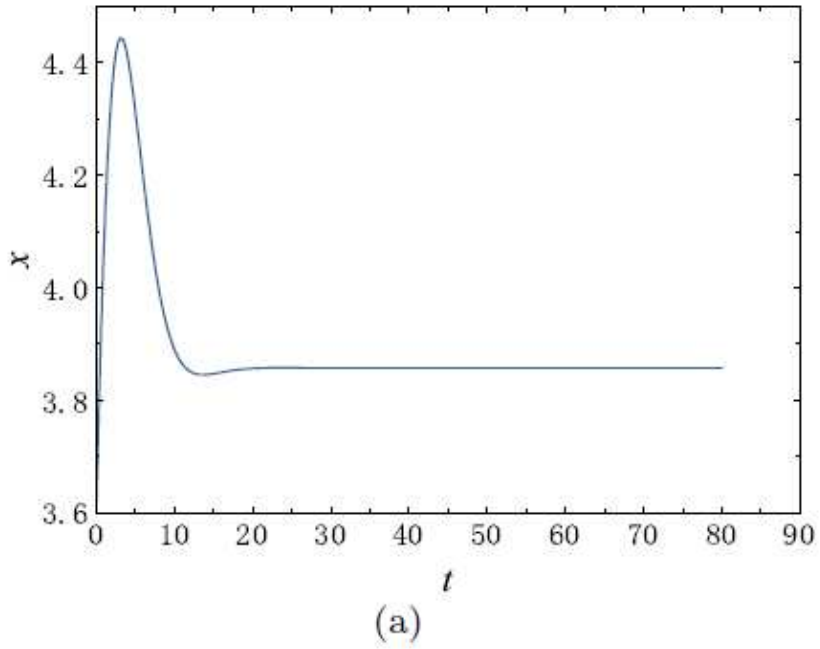

(a)

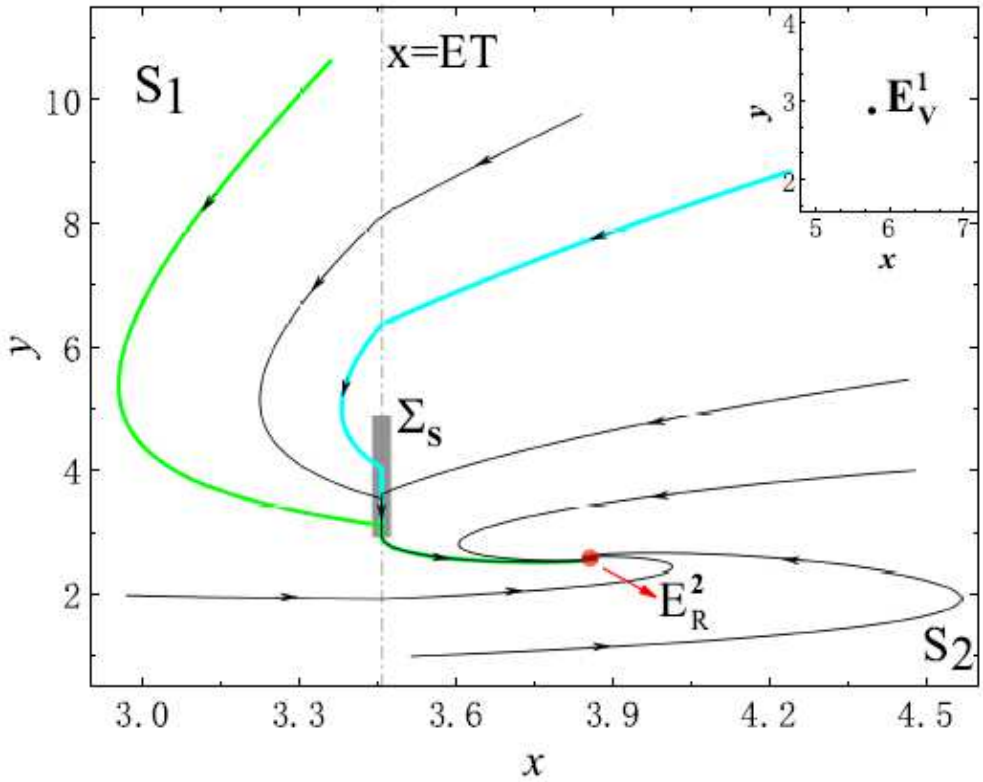

(b)

Figure 4

Please see manuscript .pdf for full caption.

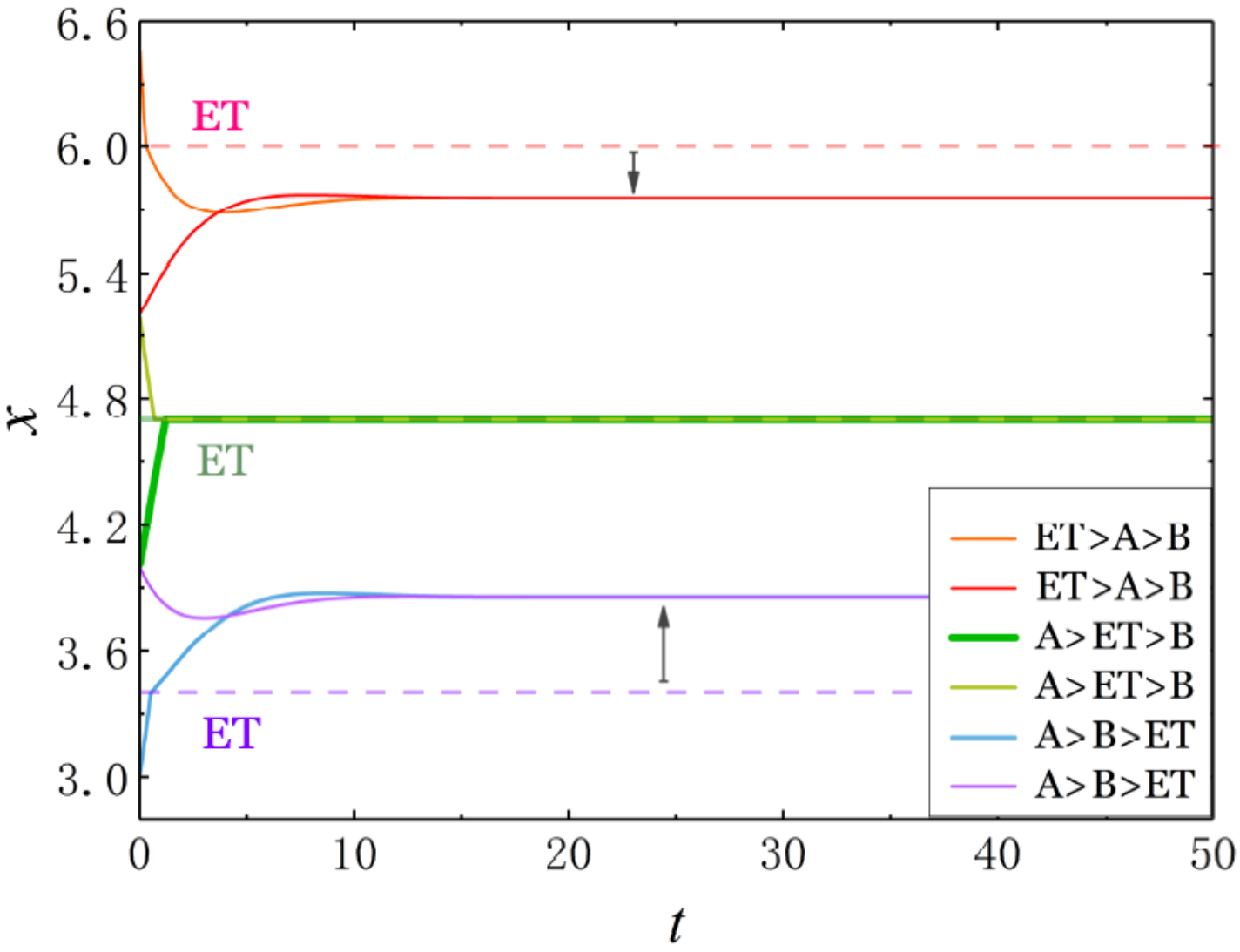

Figure 5

Please see manuscript .pdf for full caption.